

A Three-Stage Adsorption Cycle with Three Silica-Gel Beds

I Gusti Agung Bagus WIRAJATI* **† Muhammad UMAIR* Koji ENOKI*** Yuki UEDA***
Atsushi AKISAWA***

- * Bio-Applications and Systems Engineering, Tokyo University of Agriculture and Technology,
(2-24-16 Naka-cho, Koganei, Tokyo 184-8588)
** Bali State Polytechnic
(Bukit Jimbaran, Kuta Selatan, Bali 80364)
*** Institute of Engineering, Tokyo University of Agriculture and Technology,
(2-24-16 Naka-cho, Koganei, Tokyo 184-8588)

Summary

This paper proposes a three-bed three-stage adsorption cycle with a new operational strategy. The cycle consists of three adsorber/desorber heat exchangers, one evaporator, and one condenser. The two beds on the low-pressure side operate in a re-heat cycle, and another bed on the high-pressure side operates in a conventional cycle. The objectives of the current study were to evaluate the cycle at a low heat source temperature such that it can be driven by solar or waste heat and to reduce the number of heat exchangers from six beds to three beds. A simulation model was developed, and the system behavior and its performance were predicted. The performance of the proposed cycle was compared with that of a conventional six-bed three-stage adsorption cycle. The simulation results showed that the proposed cycle with the new operational strategy could operate at low heat source temperature i.e., 45 °C, and offers approximately five times higher performance in terms of SCP than the conventional cycle. Consequently, the proposed cycle is effective for use of a low-grade heat source, even with three beds.

Keywords: Adsorption cycle, Three-bed three-stage cycle, Silica gel, water, COP, SCP

1. Introduction

Heat-driven adsorption systems have become one of the most promising systems because their heat sources can be driven close to the environmental temperature during their operation. Additionally, adsorption chillers that use water and silica gel as the adsorbent-refrigerant pair show that these systems are well suited to reduction of greenhouse gas emission and consumption of low grade energy, as suggested by Kashiwagi *et al.*¹⁾

The possibility of reducing the size of the adsorber/desorber beds is also intriguing because new adsorption machines could be smaller in size than the current versions. However, heat source temperatures below 50 °C cannot be implemented, as Khan *et al.*^{2,3)}, Mizan *et al.*⁴⁾, and Wirajati *et al.*⁵⁾ have reported.

Certain researchers have investigated solutions for use of low-temperature heat sources by introducing multi-stage adsorption cycles with multiple beds⁶⁻⁹⁾. Saha *et al.*^{10,11)} simulated these systems analytically and stated that the systems could use low temperatures between 60-40 °C as the driving heat source with the application of six beds. Alam *et al.*¹²⁾ experimentally studied a re-heat two-stage system and reported that four beds could be used to exploit a heat source temperature of 55 °C.

To address the need for low heat source temperatures and smaller volume machines, which

are the focus of in recent studies, a new three-bed three-stage silica-gel adsorption cycle with a new operational strategy is introduced in this paper.

The objective of this study is to evaluate the proposed cycle in comparison with the conventional six-bed adsorption cycle. Cycle time optimization is required for a proper comparison because the cycle time always depends on the heat source temperature and the values of the physical properties of the heat exchangers. Therefore, this study aims to compare the maximized performance of both cycles in terms of specific cooling power to understand how the three-stage system works with three beds.

Nomenclature

A	area	m^2
C	specific heat	$Jkg^{-1}K^{-1}$
D_o	pre-exponential constant	m^2s^{-1}
E_a	activation energy	Jkg^{-1}
L	latent heat of vaporization	Jkg^{-1}
\dot{m}	mass flow rate	$kg s^{-1}$
P_s	saturated vapor pressure	Pa
q	amount of adsorbed water	$kg kg^{-1}$
q^*	equilibrium amount of adsorbed water	$kg kg^{-1}$
Q_s	isosteric heat of adsorption	Jkg^{-1}
R	gas constant	$Jkg^{-1}K^{-1}$
R_p	average radius of a particle	m
T	temperature	K

†Fax:+81 42-388-7282 E-mail:agungwira2@yahoo.com

t	time	s
U	overall heat transfer coefficient	$\text{Wm}^{-2}\text{K}^{-1}$
W	weight	kg
γ	bed connection indicator	-
δ	adsorption indicator	-
ε	heat exchanger efficiency	-

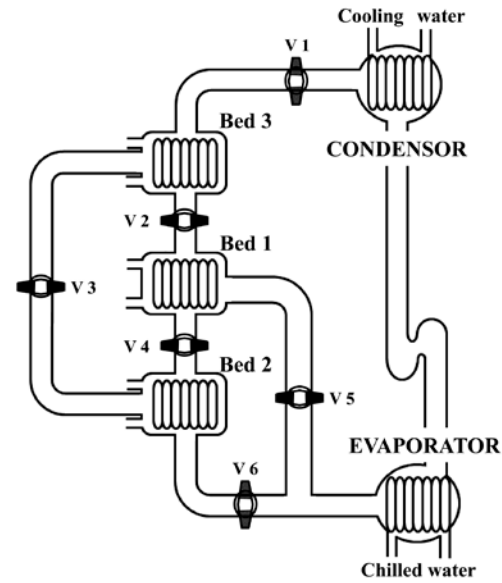
Subscripts

ads	adsorption
ads-eva	adsorbed vapor from evaporator to adsorber
bed	heat exchanger
con	condenser
ch	chilled water
cw	cooling water
cycle	cycle
des	desorption
des-con	desorbed vapor from desorber to condenser
eva	evaporator
hw	hot water
i	inlet
o	outlet
s	adsorbent
total	total
v	vapor
w	water

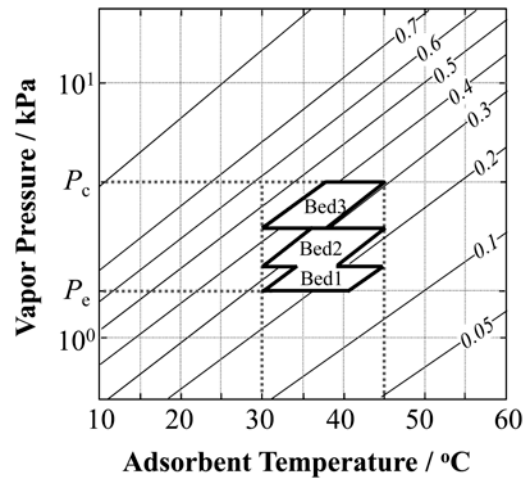
2. Three-Bed Three-Stage Adsorption Cycle Working Process.

A schematic of the three-bed three-stage adsorption cycle and its behavior are presented in Fig. 1 in the Dühring diagram, and the mode strategy of the proposed cycle is shown in Fig. 2. The cycle consists of three adsorber/desorber beds, one condenser, and one evaporator; it is assumed that silica-gel-A type is used in the cycle simulation of this study. The Dühring diagram reflects the adsorption isotherm, but the hysteresis of adsorption/desorption is neglected in the simulations, which may give rise to a factor of uncertainty. To complete a full cycle, the system operates continuously throughout eight modes.

At the beginning of the process (mode A), valves V2 and V6 are opened. Bed1 connects to Bed3, and vapor is transferred into Bed 3, which is recognized as the adsorption process for Bed3 and the desorption process for Bed1. In this mode, Bed2 connects to the evaporator, and the adsorption process begins. The desorption and adsorption processes take place at the condenser pressure (P_c) and the evaporator pressure (P_e), as shown in the Dühring diagram. During the desorption process, Bed1 is heated by hot water (Q_{des}) to the heat source temperature (T_{des}). The refrigerant vapor is cooled to the condenser temperature (T_c) by the cooling water,



(a) Schematic diagram



(b) Dühring diagram

Fig. 1 Three-bed, three-stage adsorption cycle

Bed	A	B	C	D	E	F	G	H
1	Des	Mrh	Pc	Ads	Mrc	Ph		
2	Ads	Mrc	Ph	Des	Mrh	Pc		
3	Ads	Ph	Des	Pc	Ads	Ph	Des	Pc

Ph	: Pre-heating
Pc	: Pre-cooling
Des	: Desorption
Ads	: Adsorption
Mrh	: Mass recovery heating
Mrc	: Mass recovery cooling

Fig. 2 Cycle mode operational strategy

which removes the condensation heat (Q_c). During the adsorption process, refrigerant in the evaporator is evaporated using the evaporation temperature (T_e) and seized heat (Q_e) from the chilled water. The adsorbers of Bed2 and Bed3 absorb the evaporated vapor. Then, the adsorption heat (Q_{ads}) is removed by the cooling water. When the concentration of refrigerant in all of the adsorber/desorber beds is near the equilibrium level, the process continues into mode B.

In mode B, all beds are unconnected to the condenser or evaporator. Bed1 is positioned at the end position of desorption process and the other beds (Bed2 and Bed3) at the end position of the adsorption process. Bed1 is connected with Bed2 through valve V4 with continuous cooling water in Bed2 and hot water in Bed1. The Bed2 cooling process is referred to as mass recovery cooling, and the heating process of Bed1 is known as mass recovery heating. During these processes, vapor is transferred from Bed1 to Bed2. If the pressure of both Bed1 and Bed2 are nearly equal, then the process continues to mode D. In mode B, Bed3 is heated by hot water in the pre-heating process. If the pressure of Bed3 is nearly equal to the condenser pressure, then the process continues to mode C in which valve V1 is opened, and the desorption process for Bed3 begins.

In mode D, all beds are included in the pre-heating or pre-cooling process. Bed1 and Bed3 are cooled by cooling water in the pre-cooling process, and Bed2 is heated by hot water in the pre-heating process. If the pressures of Bed1 and Bed3 are nearly equal to the pressure of evaporator and the pressure of Bed2 is nearly equal to the pressure of the condenser, then valves V3 and V5 are opened to refrigerant flow. Bed2 and bed3 are now connected, and Bed1 is connected with the evaporator.

Mode D occurs at the end of the half cycle of the process. To complete a full cycle, the next process is the same as the previous half-cycle referred to in the mode operational strategy of Fig. 2.

In this cycle, the pressure rise from the evaporator level to the condenser level is split into three progressive smaller pressure rises, as seen in Fig. 1(b). Bed1 and Bed2 pressurize the vapor from the evaporation level to the intermediate level. Next, Bed3 pressurizes the vapor from the intermediate level to the condensation level.

3. Mathematical Modeling

3.1 Adsorber/desorber energy balance

The heat transfer equation for the adsorbent beds can be described as follows:

$$T_o = T + (T_i - T) \exp\left(\frac{U_{bed} A_{bed}}{\dot{m}_w C_w}\right) \quad (1)$$

where T denotes the bed temperature. The adsorbent bed temperature, pressure, and concentration of water content are assumed uniform throughout the adsorbent bed. The heat transfer fluid (water) temperature parameters T_i and T_o denote the cooling water upon adsorption and the hot water upon desorption, respectively.

The energy balance equation of adsorbent beds is shown below:

$$\begin{aligned} (W_s C_s + W_w C_w q + W_{bed} C_{bed}) \frac{dT}{dt} &= W_s Q_s \frac{dq}{dt} \\ - W_s C_w \delta [\gamma (T - T_{eva}) + (1 - \gamma) (T - T_{ww})] & \frac{dq}{dt} \\ + \dot{m}_w C_w \varepsilon_{bed} (T_i - T) & \end{aligned} \quad (2)$$

where δ is either 0 or 1 depending on whether the adsorbent bed is working as a desorber or adsorber, and γ is either 1 or 0 depending on whether the bed is connected with the evaporator or another bed. Equation (1) expresses the importance of the heat transfer parameters, namely, the heat transfer area A_{bed} and overall heat transfer coefficient U_{bed} . The left-hand side of the adsorber/desorber energy balance equations (Eq. (2)) provides the amount of sensible heat required to cool or heat the silica-gel (s), water (w) as well as the metallic (bed) components of the heat exchanger during adsorption or desorption in a batched-cycle operation. The first term on the right-hand side of Eq. (2) constitutes the release of adsorption heat or the input of desorption heat, and the second term denotes the sensible heat of the adsorbed vapor. The last term on the right-hand side of Eq. (2) refers to the total amount of heat released to the cooling water upon adsorption or provided by the hot water for desorption. Equation (2) does not account for external heat losses to the environment because all of the beds are considered well insulated. The term ε_{bed} in Eq. (2) expresses the heat exchanger effectiveness of the adsorbent.

3.2 Evaporator energy balance

Equation (3) and Eq. (4) represent the heat transfer of evaporator and the energy balance of the evaporator, respectively as follows:

$$T_{ch,o} = T_{eva} + (T_{ch,i} - T_{eva}) \exp\left(-\frac{U_{eva} A_{eva}}{\dot{m}_{ch} C_{ch}}\right) \quad (3)$$

$$\begin{aligned} (W_{eva,w} C_w + W_{eva,bed} C_{eva,bed}) \frac{dT_e}{dt} &= \dot{m}_{ch} C_{ch} \varepsilon_{eva} \\ (T_{ch,i} - T_{eva}) - W_s \left(\frac{dq_{ads-eva}}{dt} + \frac{dq_{des-con}}{dt} \right) & (L + C_v (T_{con} - T_{eva})) \end{aligned} \quad (4)$$

The left-hand side of Eq. (4) represents the sensible heat requirement for the liquid refrigerant and the metal of the heat exchanger in the evaporator. The first term on the right-hand side of Eq. (4) represents the total amount of heat from the chilled water, and the second term accounts for the latent heat of vaporization (L) for the amount of refrigerant adsorbed (dq_{ads}/dt) and the sensible heat required to cool the incoming condensate from the condensation temperature T_{con} to the evaporation temperature T_{eva} . The term ε_{eva} in Eq. (4) expresses the heat exchanger effectiveness.

3.3 Condenser energy balance

Equation (5) represents the heat transfer of the condenser, and Eq. (6) describes the energy balance for the condenser expressed as:

$$T_{con,o} = T_{con} + (T_{cw,i} - T_{con}) \exp\left(-\frac{U_{con} A_{con}}{\dot{m}_{cw} C_w}\right) \quad (5)$$

$$\begin{aligned} (W_{con,w} \cdot C_w + W_{con,bed} \cdot C_{con,bed}) \frac{dT_c}{dt} &= \dot{m}_{cw} C_w \varepsilon_{con} \\ (T_{cw,i} - T_{con}) - W_s \left(\frac{dq_{des-con}}{dt}\right) & (L + C_v (T_{des} - T_{con})) \end{aligned} \quad (6)$$

The left-hand side of Eq. (6) represents the sensible heat required by the metallic components of the heat exchanger due to the temperature variations in the condenser. The first term on the right-hand side of Eq. (6) indicates the amount of heat released to the cooling water, and the second term accounts for the latent heat of condensation (L) for the amount of refrigerant desorbed (dq_{des}/dt) and the amount of heat that the liquid condensate carries away when it leaves the condenser for the evaporator. The term ε_{con} in Eq. (6) denotes the heat exchanger effectiveness.

3.4 Total mass balance

The total mass balance of the refrigerant (water) can be expressed as:

$$W_{eva,w} = -W_s \left(\frac{dq_{des-con}}{dt} + \frac{dq_{ads-eva}}{dt}\right) \quad (7)$$

where the subscripts of des-con and ads-eva refer to the vapor flow from the desorber to the condenser and from the evaporator to the adsorber, respectively.

3.5 Adsorption rate

The adsorption rate of the silica gel is described in many studies, i.e., Sakoda *et al.*¹³⁾:

$$dq/dt = k_s a_p \cdot (q^* - q) \quad (8)$$

The overall mass transfer coefficient $k_s a_p$, is estimated using Eq. (9) and (10).

$$k_s a_p = \frac{15D}{R_p^2} \quad (9)$$

$$D = D_0 \exp(-E_a/RT) \quad (10)$$

The amount of refrigerant adsorbed at equilibrium q^* is predicted by the equation as follows:

$$q^* = \frac{0.8 [P_s(T_w)/P_s(T_s)]}{1 + 0.5 [P_s(T_w)/P_s(T_s)]} \quad (11)$$

where $P_s(T_w)$ and $P_s(T_s)$ are the saturation vapor pressure at temperature T_w (water vapor) and T_s (silica gel), respectively. The saturation vapor pressure and temperature are correlated by Antoine's equation as shown below:

$$P_s = 133.32 \exp\left(18.3 - \frac{3820}{T - 46.1}\right) \quad (12)$$

3.6 System performance

The coefficient of performance (COP) and specific cooling power (SCP), which are the main performance characteristics of the adsorption refrigeration cycles, are measured as:

$$\begin{aligned} \text{COP} &= \dot{m}_{ch} C_w \int_0^{t_{\text{cycle}}} (T_{ch,i} - T_{ch,o}) \\ & / C_w \int_0^{t_{\text{cycle}}} (T_{hw,i} - T_{hw,o}) dt \end{aligned} \quad (13)$$

$$\begin{aligned} \text{SCP} &= \dot{m}_{ch} C_w \int_0^{t_{\text{cycle}}} (T_{ch,i} - T_{ch,o}) \\ & / t_{\text{cycle}} W_{s,\text{total}} \end{aligned} \quad (14)$$

The values of the physical property parameters used in the calculations and the standard operating conditions adopted in the simulation are listed in Table 1 and Table 2, respectively. Certain values in Table 1, i.e., UA_{ads} , UA_{con} , and UA_{eva} , are adopted from Khan *et al.*²⁾. The amount of adsorbent in every bed is 16 kg.

4. Results and Discussion

A complete simulation program was developed based on MATLAB software and used to solve all of the equations. Once all of the input parameters (i.e., adsorbent-refrigerant properties, flow rates of heat transfer fluids, and specifications of heat exchangers) are initially given, the cyclic operation can be simulated.

Particle Swarm Optimization (PSO)⁴⁾ is used to optimize the cycle time in terms of SCP, which was

Table 1 Values of physical parameters²⁾

Symbol	Value	Unit
C_{bed}	20×10^3	$J \cdot kg^{-1} \cdot K^{-1}$
C_s	924	$J \cdot kg^{-1} \cdot K^{-1}$
C_v	1.89×10^3	$J \cdot kg^{-1} \cdot K^{-1}$
C_w	4.18×10^3	$J \cdot kg^{-1} \cdot K^{-1}$
D_o	2.54×10^{-4}	$m^2 \cdot s^{-1}$
E_a	2.33×10^6	$J \cdot kg^{-1}$
L_w	2.50×10^6	$J \cdot kg^{-1}$
Q_s	2.80×10^6	$J \cdot kg^{-1}$
R	4.62×10^2	$J \cdot kg^{-1} \cdot K^{-1}$
R_p	3.00×10^{-4}	m
UA_{ads}	2.00×10^3	$W \cdot m^{-2} \cdot K^{-1}$
UA_{con}	4.06×10^3	$W \cdot m^{-2} \cdot K^{-1}$
UA_{eva}	2.36×10^3	$W \cdot m^{-2} \cdot K^{-1}$
W_{bed}	12	kg
$W_{con,w}$	5	kg
$W_{eva,w}$	25	kg
W_s	16	kg

Table 2 Standard operating conditions

	Temperature °C		Flow Rate $kg \cdot s^{-1}$
Hot water	45-50		1
Cooling water	30		1(ads) + 0.5(des)
Chilled water	Inlet	14	0.1 (45 °C), 0.2 (50 °C)
	Outlet	9	

chosen as the objective function to be maximized, and the cycle time components (i.e., adsorption/desorption time, pre-cooling/pre-heating time, and mass recovery time) were chosen as the variables. In PSO, the particles contain the values of the variables, and the algorithm updates the values toward the optimal solution. After a number of updating calculations, all of the particles contain the same value, and the objective function achieves a maximized value. In this case, the number of particles and the number of iterations were 20 and 500, respectively. It was observed that all particles reached their best position prior to 500 iterations. Because the main objective is to use a low heat source temperature (i.e., less than 60 °C), the investigation was conducted for hot water temperatures of 45°C and 50 °C.

4.1 Temperature histories of the adsorber/desorber beds

Figure 3 illustrates the temperature histories of the three-bed cycle with a heat source temperature of 45 °C.

In the beginning of the process (mode A), the desorption process for Bed1 and the adsorption processes for Bed2 and Bed3 were carried out with increasing and decreasing temperatures, respectively. In this process, Bed2 and Bed3 operated at the evaporator pressure, and Bed1 operated at the condenser pressure. In mode B, Bed3 was operated in the pre-heating process, and thus, the temperature of Bed3 increased because Bed3 was heated by hot water and continued into mode C such that Bed3 was switched into the desorption process. In modes B and C, Bed1 and Bed2 were in the mass recovery state with heating and cooling and temperature changes accordingly. During mode D, the temperature of Bed1 and Bed3 decreased, and the temperature of Bed2 increased due to cooling by the cooling water and heating by the hot water. Mode D occurred at the end of the half cycle. The temperature behavior of the remaining cycle was the same as in the previous cycle.

4.2 Water content in bed

Figure 4 illustrates the variation of the water content in adsorber/desorber of the beds for the full

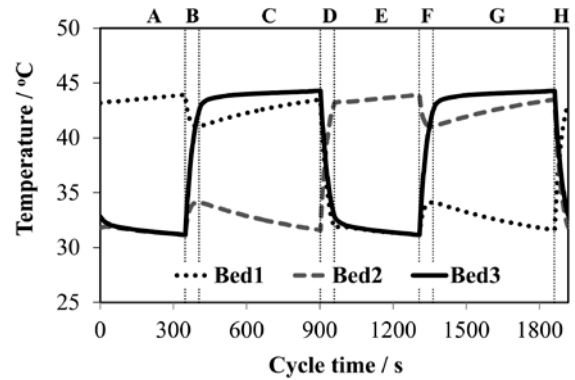


Fig. 3 Temperature histories of the adsorber/desorber beds

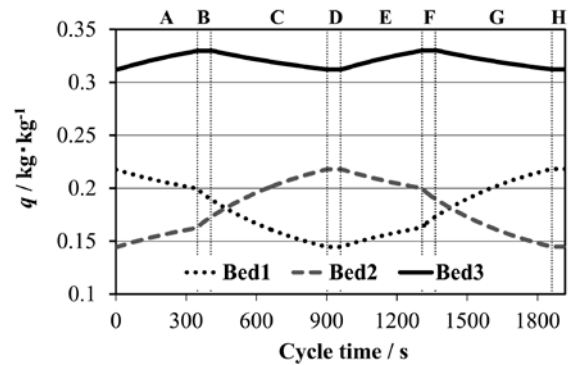


Fig. 4 Variations of water content in the adsorbent

cycle.

The water content in the Bed1 decreased during the desorption process because the vapor was transferred into Bed3 in mode A, whereas that of Bed2 increased because the bed adsorbed vapor from the evaporator. During the pre-heating and pre-cooling processes, the water content in all of the beds remained constant because all valves in the system were fully closed (i.e., mode B for Bed 3 and mode D for Bed1 and Bed2). In mass recovery with heating process (mode B-C), the water content in Bed1 decreased because the vapor was transferred into Bed2. In the mass recovery with cooling process, the water content in Bed2 increased because it received vapor from Bed1.

During mode A, Bed1 was connected to Bed3, and during mode E, Bed2 was connected to Bed3, where the vapor from the evaporator was consequently transferred from the lower pressure side to Bed3. In these cases, Bed3 worked continuously to send vapor from the intermediate pressure to condensation pressure, and a full cycle was properly completed.

4.3 Cycle time optimization

Cycle time optimization was conducted to compare the performances of the proposed cycle and the conventional six-bed three-stage cycle, which Saha *et al.*¹¹⁾ proved could work with low heat source temperature. The preferable cycle time depends on the cycle configuration, heat exchanger profile, and heat source temperature. To compare the cycles properly, the cycle time should be selected to maximize the performance. In this work, each cycle time for the two cycles was optimized in terms of the specific cooling power.

The results of the optimized cycle time allocation of the three-bed three-stage cycle and the six-bed three-stage cycle are presented in Table 3. The results indicate that a longer cycle time is required for both cycles if the heat source temperature is 45 °C rather than 50 °C. The increment between the two temperature cases results from the expansion of the adsorption/desorption process and the mass

Table 3 Comparison of optimized cycle time allocation level

Adsorption Cycle	Heat Source °C	Time s			Total Time s
		Ads/Des	Ph/Pc	Mrc/Mrh	
3 Bed 3 Stage	45	696	113	1106	1915
	50	407	95	850	1392
6 Bed 3 Stage	45	1008	113	0	1121
	50	902	108	0	1010

recovery process. From the viewpoint of total cycle time, the proposed cycle requires a cycle time that is 1.4-1.7 times longer than that of the conventional cycle.

The performance comparison of the proposed cycle at two different heat source temperatures is shown in Fig. 5. It is apparent that the current cycle can operate at a low heat source temperature of 45 °C, and the chilled water outlet was held constant at 9 °C. Based on Fig. 5, the performance increased with the heat source temperature. The performances of both COP and SCP of the proposed cycle are superior to those of the six-bed conventional three-stage cycle. Although the same amount of silica gel was packed in each bed, the performance of the proposed cycle was almost two times higher than that of the conventional 6-bed process. Because the proposed cycle uses half the amount of silica gel compared with the conventional six-bed cycle, the proposed cycle is advantageous in terms of SCP. The proposed cycle has also produces an SCP value that is approximately 5 times higher than that of the conventional cycle.

From this point of view, the three-bed three-stage cycle with the new operational strategy is promising because it can exploit low temperature heat sources. Furthermore, the proposed method also

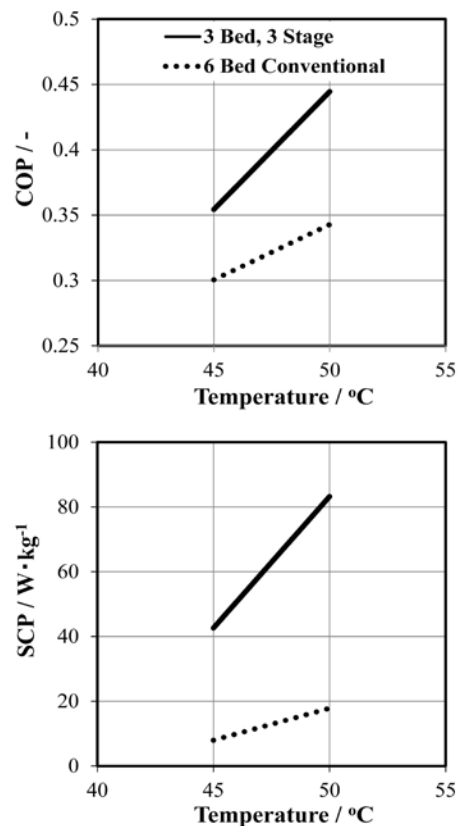


Fig. 5 Comparison of performances between the proposed cycle and conventional cycle

provides the potential to produce more compact three-stage adsorption machines by reducing the number of adsorber/desorber heat exchangers.

5. Conclusion

A simulation study of a three-bed three-stage adsorption cycle was carried out with cycle time optimization to evaluate the system performance. The ability to exploit a low heat source temperature and reduce bed utilization is the highlight of the examinations in this study. The simulation results showed that the proposed cycle with the new operational strategy could operate with a low heat source temperature of 45 °C, which offers approximately five times higher performance in terms of SCP than the conventional six-bed three-stage adsorption cycle. Consequently, this work emphasizes that the proposed cycle is effective for utilization of a low-grade heat source even with three beds.

References

- 1) Kashiwagi, T., Akisawa, T., Yoshida, S., Hamamoto, Y. and Alam, K.C.A., Proc. of the International Sorption Heat Pumps Conference, Shanghai, China (2002), pp.50-62.
- 2) Khan, M.Z.I., Alam, K.C.A., Saha, B.B., Hamamoto, Y., Akisawa, A. and Kashiwagi, T., Parametric study of a two-stage adsorption chiller using re-heat—The effect of overall thermal conductance and adsorbent mass on system performance, *Int. Journal of Thermal Science*, 2006, **45** (5), pp. 511–519.
- 3) Khan, M.Z.I., Saha, B.B., Alam, K.C.A., Akisawa, A. and Kashiwagi, T., Study on solar/waste heat driven multi-bed adsorption chiller with mass recovery, *Renew. Energy*, 2007, **32** (3), pp. 365–381.
- 4) Mizanur Rahman, A. F. M., Ueda, Y., Akisawa, A., Miyazaki, T. and Saha, B. B., Performance Comparison of Three-Bed Adsorption Cooling System With Optimal Cycle Time Setting, *Heat Transfer Engineering*, 2013, **34** (11-12), pp. 938-947.
- 5) IGAB Wirajati, Ueda, Y., Akisawa, A. and Miyazaki, T., Proc. of the International Sorption Heat Pumps Conference, Washington, USA (2014), No.7.
- 6) El-Sharkawy, I.I., AbdelMeguid, H. and Saha, B.B., Towards an optimal performance of adsorption chillers: Reallocation of adsorption/desorption cycle times, *International Journal of Heat and Mass Transfer*, 2013, **63**, pp. 171–182.
- 7) Habib, K., Coudhury, B., Chatterjee, P.K. and Saha, B.B., Study on a solar heat driven dual-mode adsorption chiller, *Energy*, 2013, **63**, pp. 133-141.
- 8) Miyazaki, T., Akisawa, A. and Saha, B.B., The performance analysis of a novel dual evaporator type three-bed adsorption chiller, *International Journal of Refrigeration*, 2010, **33**, pp. 276–285.
- 9) Miyazaki, T., Akisawa, A., Saha, B.B., El-Sharkawy, I.I. and Chakraborty, A., A new cycle time allocation for enhancing the performance of two-bed adsorption chillers, *International Journal of Refrigeration*, 2010, **32** (5), pp. 846–853.
- 10) Saha, B. B., Akisawa, A. and Kashiwagi, T., Silica gel water advanced adsorption refrigeration cycle, *Energy*, 1997, **22** (4), pp. 437–447.
- 11) Saha, B. B., Koyama, S., Kashiwagi, T., Akisawa, A., K.C. Ng and H.T. Chua, Waste heat driven dual-mode, multi-stage, multi-bed regenerative adsorption system, *Int. Journal of Refrigeration*, 2003, **26** (7), pp. 749-757
- 12) Alam, K.C.A., Khan, M.Z.I., Uyun, A.S., Hamamoto, Y., Akisawa, A. and Kashiwagi, T., Experimental study of a low temperature heat driven re-heat two-stage adsorption chiller, *Applied Thermal Engineering*, 2007, **27** (10), pp. 1686–1692.
- 13) Sakoda, A. and Suzuki, Fundamental study on solar powered adsorption, *Journal of Chemical Engineering of Japan*, 1984, **17** (1), pp.52-57.